OPEN ACCESS



ISAR Journal of Science and Technology

Volume 4, Issue 8, 2026, Page: 60-76

Abbriviate Title- ISAR J Sci Tech

ISSN *(Online)*- 2584-2056

https://isarpublisher.com/journal/isarjst

ANALYSIS OF THE RELATIONSHIP OF AEROSOL OPTICAL PROPERTIES AND MICROPHYSICAL PARAMETERS WITH RELATIVE HUMIDITY FOR URBAN AEROSOLS

K. U. Yarima[1]*, B. I. Tijjani[2], M. Idris[3] and A. Aliyu[4]

[1,2,3] Department of Physics, Bayero University Kano. PMB 3011 Kano State, Nigeria.

[4]Department of Physics, Aliko Dangote University of Science and Technology Wudil, Kano State, Nigeria.

***Corresponding Author**

K. U. Yarima

E-mail:
khamisuyerima01@gmail.com

Article History

Received: 14.06.2026
Revised: 10.07.2026
Accepted: 06.08.2026
Published: 26.08.2026

Abstract: This study quantifies how particle chemistry and relative humidity (RH) jointly control the Ångström exponent (α) and turbidity coefficient (β) of urban aerosols, using OPAC 4.0 simulations validated against 1997–2010 MODIS retrievals over ten regions. α is shown to diagnose the humidity-modified extinction size mode, while β measures aerosol loading. OPAC varied water-soluble (WASO), insoluble (INSO), and soot fractions across five concentrations and eight RH levels (0–99%). The key finding is that the optical response is governed by the balance between the Raoult (water activity) and Kelvin terms, with composition setting its magnitude: the soluble fraction amplifies the response, while insoluble and soot fractions suppress it. Although the Kelvin term rises with WASO and RH (via surface-tension enhancement by dissolved salts), it never reverses Raoult-driven growth, so α falls and β rises with humidity for all types. For the most soluble WASO model, α drops from 1.47 to 1.03 with β rising 13-fold, versus 1.13→1.01 (7-fold) for INSO and 1.39→1.08 (5-fold) for soot. Satellite data match OPAC only within the urban α range (≈1.00–1.47): Germany (α = 1.27) and Serbia (α = 1.00) agree to within 0.01 at 90 % and 99 % RH, though β is over-predicted 7–10-fold. The other eight regions fall outside the urban envelope, spanning dry soluble-rich aerosol (Ethiopia, α = 1.45), fresh biomass burning (USA, α = 1.84; South Africa, α = 2.39), and coarse dust or dust–pollution mixtures (France, India, Mexico, Nigeria, Egypt; α = 0.12–0.85). These results provide a composition-resolved framework for interpreting satellite aerosol products in terms of hygroscopic state, with implications for radiative forcing and aerosol–cloud parameterisations.

Keywords: Ångström exponent (α), Hygroscopic growth factor, Kelvin effect, Turbidity coefficient (β), Water activity.

This work is licensed under a Creative Commons Attribution-NonCommercial 4.0 International License (CC BY-NC 4.0)

Cite this article:

Yarima, K. U., Tijjani, B. I., Idris, M., and Aliyu, A., (2026). ANALYSIS OF THE RELATIONSHIP OF AEROSOL OPTICAL PROPERTIES AND MICROPHYSICAL PARAMETERS WITH RELATIVE HUMIDITY FOR URBAN AEROSOLS. *ISAR Journal of Science and Technology*, *4*(8), 60-76.

1.0 Introduction

Atmospheric aerosols constitute a major uncertainty in climate assessments, directly influencing Earth's radiative budget through scattering and absorption (Stocker *et al*., 2013). Urban aerosols exhibit particular complexity due to heterogeneous sources: fossil fuel combustion, industrial activities, biomass burning, and resuspended mineral dust. Each component manifests distinct optical characteristics INSO (mineral dust) shows weak spectral dependence, SOOT demonstrates strong absorption, and WASO components (sulfates, nitrates, organics) undergo pronounced hygroscopic growth (Seinfeld & Pandis, 2016).

The interaction between aerosols and water vapor critically alters optical properties as hygroscopic particles absorb water with increasing RH, shifting phase functions toward stronger forward scattering (Svenningsson *et al*., 2006). However, this response varies non-linearly with concentration and chemical species.

The OPAC software package (Hess *et al*., 1998; Koepke *et al*., 2015) enables computation of spectral optical properties for user-defined aerosol mixtures. Despite its widespread application, the following research gaps persist: 1 component-specific Angostrom Exponent response to RH across concentration gradients remains unquantified; 2 validation against satellite-derived α across diverse geographical regions is limited; and

This study addresses these gaps by: 1 numerically evaluating concentration and RH effects on hygroscopic growth, Kelvin Effect, Water Activities and Angostron exponent using the microphysical properties extracted from OPAC 4.0 and deriving components-specific Angostrom exponent value 2 validating the simulated Angostrom exponent against MODIS satellite retrievals across ten countries spanning dust-dominated, biomass-burning, and anthropogenic ally-influenced aerosol regimes to determine which countries comply with the theoretically simulated data.

2.0 Materials and Methods

Here, we presents the fundamental equations governing aerosol size distribution, Kelvin effect, water activity, hygroscopic growth, and the Ångström power law used in this work.

2.1 AEROSOL SIZE DISTRIBUTION

Atmospheric aerosols follow a multimodal lognormal distribution (Whitby and McMurry, 1997):

The number size distribution is:

$$\frac{dN(r)}{dLog(r)} = \sum_{i=1}^{n} \left\{ \left[\frac{N_i}{(\sqrt{2\pi})\log\sigma_i} \right] \varepsilon \exp \left[- \frac{\left[\log(r) - \log(r_{mi})\right]^2}{2\log\sigma_i^2} \right] \right\} \quad (1)$$

where r is the particle radius, r_{mi} and σ_i are mode radius and the standard deviation respectively of the i^{th} mode and N_i its total number density. For *i*=1, 2, 3 may represent mono-, bi-, or trimodal distributions.

But generally atmospheric aerosols usually comprise mixtures of soluble and insoluble components, therefore the information on the hygroscopicity modes was merged into an "over-all" or "bulk" or "effective" hygroscopic growth factor of the mixture, $g_{eff}(S)$, representative for the entire aerosols particles population (Meyer *et al*., 2009, Stock *et al*., 2011):

$$g_{eff}(S) = \left(\sum_k x_k g_k^3(S)\right)^{1/3} \quad (2)$$

where the summation is performed over all compounds present in the particles and x_k represent their respective volume fractions, using the Zdanovskii-Stokes-Robinson relation.

The growth of droplets is controlled by two opposing forces: the curvature effect (Kelvin effect) and the solute effect (Raoult's law). As supersaturation increases, aerosol particles grow through water vapor condensation, and once they exceed a critical size (critical diameter), spontaneous growth occurs. According to Kohler theory" (Kohler, 1936, Pruppacher & Klett, 1997, Seinfeld & Pandis, 2016), the condition necessary for an aqueous solution droplet to be in equilibrium with water vapor in the surrounding gas phase can be expressed as follows (Kreidenweis *et al*., 2005, Gysel *et al*., 2002):

$$S = a_w K_e \quad (3)$$

where a_w is the activity of water in the aqueous solution or Raoult term, and K_e is the Kelvin effect, which can also be described the enhancement of the equilibrium water vapor pressure due to surface curvature (Ruehl *et al*., 2010).

2.2 ÅNGSTRÖM POWER LAW

The spectral dependence extinction coefficients with wavelength is characterized by Angstrom, (1961):

$$\sigma_{ext}(\lambda) = \beta\lambda^{-\alpha} \quad (4)$$

where α (Ångström exponent) indicates particle size (larger α = fine-mode dominance) and *β* (turbidity coefficient) represents aerosol loading (Moorthy *et al*., 2001). Thus α and β carry information about particle size and amount, both of which are strongly modified by relative humidity (RH) and aerosol composition.

The Angstrom exponents were obtained as a coefficient of the following regression, of Equation (1) when linearized as

$$\ln\sigma_{ext}(\lambda) = \ln(\beta) - \alpha\ln(\lambda), \quad (5)$$

2.3 OPAC 4.0 NUMERICAL SIMULATIONS

In OPAC, urban aerosols comprise of three components; (i) water insoluble INSO (ii) water soluble WASO and (iii) SOOT.

The water-insoluble (INSO) component consists mainly of soil-derived mineral particles. The water-soluble (WASO) component comprises sulphates, nitrates, and other species that readily dissolve in water and are strongly hygroscopic. Soot represents fresh black carbon, which is hydrophobic and does not take up water with rising RH, its growth factor remaining near unity (Weingartner et al., 1997; Hess et al., 1998). In OPAC, soot therefore acts as a non-hygroscopic diluent: increasing soot concentration reduces the soluble volume fraction and suppresses the effective growth of the population, even though soot itself does not grow. Aged, coated soot can become hygroscopic, but this is not represented in the OPAC urban model.

OPAC 4.0 computed optical properties across the visible spectrum (0.4–0.8 µm) for fifteen aerosol models (Tables 1-3). Five concentration gradients per component (INSO, SOOT, WASO) were simulated at 0, 50, 70, 80,90, 95, 98, and 99% RH.

The models (mixtures) of the aerosols used in the simulation in OPAC 4.0 are given in Tables 1, 2 and 3. The number densities were increased by adding 30% of the initial concentrations.

Table 1: The Concentrations of the Aerosols with varying Concentrations of **INSO**.

Components	Number densities (cm^{-3})					
INSO	**1.5**	**1.95**	**2.535**	**3.2955**	**4.28415**	**5.569395**
WASO	28000	28000	28000	28000	28000	28000
SOOT	130000	130000	130000	130000	130000	130000

Table 2: The Concentrations of the Aerosols with varying Concentrations of **WASO**.

Components	Number densities (cm^{-3})					
INSO	1.5	1.5	1.5	1.5	1.5	1.5
WASO	**28000**	**36400**	**47320**	**61516**	**79970.8**	**103962**
SOOT	130000	130000	130000	130000	130000	130000

Table 3: The Concentrations of the Aerosols with varying Concentrations of **SOOT**.

Components	Number densities (cm^{-3})					
INSO	1.5	1.5	1.5	1.5	1.5	1.5
WASO	28000	28000	28000	28000	28000	28000
SOOT	**130000**	**169000**	**219700**	**285610**	**371293**	**482680.9**

2.4 MODIS SATELLITE DATA VALIDATION

The ten countries in Table 4 were selected based on strategic representation of diverse global aerosol regimes to rigorously test the validity of OPAC 4.0 simulations across varying atmospheric conditions. The selection rationale encompasses:

Table 4: **Geographical Bounding Boxes for MODIS Aerosol Product Extraction**

Country	**Location**	**Long. Coordinate**	**Lat. Coordinate**	**Dominant Aerosols Type**
South Africa	Johannesburg	28.044°E	26.202°S	Biomass burning
USA	New York	74.006°W	40.713°N	Urban-Industrial/biomass
Ethiopia	Addis-Ababa	38.747°E	9.025°N	Mixed biomass/dust
Germany	Berlin	13.400°E	52.520°N	Urban-Industrial
Serbia	Belgrade	20.457°E	44.787°N	Mixed urban/dust
India	Delhi	77.231°E	28.652°N	Anthropogenic/dust

France	Paris	2.349°E	48.853°N	Marine/Urban
Mexico	Mexico City	99.130°W	19.430°N	Mixed urban/biomass/dust
Nigeria	Lagos	3.395°E	6.454°N	Dust/biomass
Egypt	Cairo	31.235°E	30.044`°N	Saharan Dust

The countries span four dominant aerosol categories: Biomass burning-dominated: South Africa (savanna fires), USA (seasonal wildfires), Mineral dust-dominated: Egypt (Saharan dust), Nigeria (Sahelian dust transport), Urban-industrial: Germany, France, Serbia (fossil fuel combustion, secondary aerosols), Mixed anthropogenic/dust: India, Ethiopia, Mexico (transitional regimes).

This classification follows the aerosol typing framework established by, who demonstrated that MODIS Collection 6.1 products enable reliable discrimination of dust, biomass burning, and anthropogenic aerosols through multi-wavelength AOD and Ångström exponent analysis.

MODIS Collection 6.1 Level-2 aerosol products (MOD04/MYD04) were obtained for ten countries. Monthly mean AOD at 0.41, 0.47, 0.55, and 0.67 μm was extracted within defined bounding boxes. These MODIS Dark Target bands were selected based on three principles: the Ångström power law, τ(λ) = β λ^(−α), requiring multiple wavelengths to retrieve α and β; Mie scattering, where the blue-to-red span maximises size sensitivity; and spectral window selection, ensuring minimal gas absorption. The Ångström exponent (α) and turbidity coefficient (β) were derived by linear regression of ln τ on ln λ (Equation 5) using SPSS 22.0.

3.0 Results and Discussions

This section discusses the analysis of the results obtained from the simulations in the OPAC 4.0 and comparing with the satellite data extracted.

3.1 OPAC SIMULATED RESULTS

This subsection discuss the results obtained from the OPAC simulations.

WASO

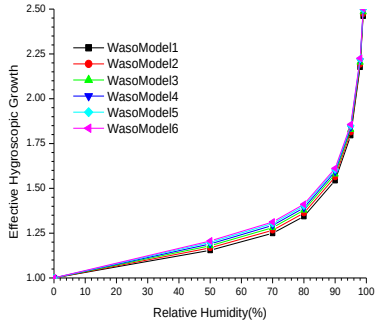


Figure 1: The Effective hygroscopic growth of waso with Relative Humidity

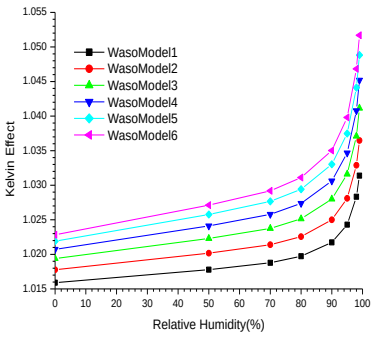


Figure 2: The Kelvin Effect of waso with Relative Humidity

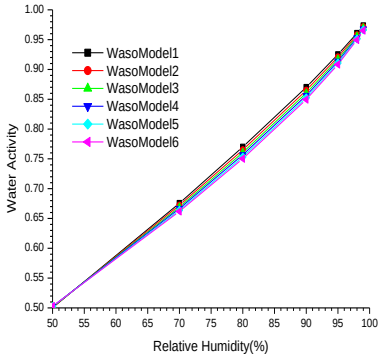


Figure 3: The water activity of waso with Relative Humidity

From Figure 1 it can be seen that at any RH > 0%, **Model 6 shows the largest growth factor, Model 1 the smallest**. This directly reflects that the more the water-soluble fraction the more soluble material and the lower equilibrium vapour pressure (Raoult effect), and this will cause more water condenses at the same RH. Below ~80% RH the growth is modest Growth Factor is less than 1.4. Above 90% the curves rise steeply. At 99% RH, all particles have more than doubled their dry diameter. This steep rise is the Raoult effect dominating over the Kelvin effect, exactly as Köhler theory predicts. The soluble salts and hygroscopic organics cause substantial water uptake as the atmosphere approaches saturation.

Figure 2 shows the Kelvin term rising with WASO concentration and RH (Model 6 highest, Model 1 lowest). This contradicts the size-only expectation, since larger droplets should give a smaller Kelvin term. The reversal occurs because soluble salts raise surface tension, which outweighs the size effect. Surface tension is therefore a key control on soluble aerosol growth.

From figure 3, it can be seen that for all the models, water activity increases with RH, approaching 1 near saturation. This is expected because the higher the RH the more water condenses and the more solution becomes more dilute and this makes water activity to become closer to 1. From the figure it can also be seen that model 1 is the most soluble particle because it has the highest water activity.

Table 5: **WASO First Model**

RH(%)	R^2	Sig	Beta	Sig	Alpha	Sig
0	.999001	9.17E-12	.084632	3.31E-15	1.372888	9.17E-12
50	.998444	4.33E-11	.113952	3.96E-14	1.378805	4.33E-11
70	.998165	7.71E-11	.133323	1.14E-13	1.369234	7.71E-11
80	.997828	1.39E-10	.155046	3.25E-13	1.353018	1.39E-10
90	.997214	3.32E-10	.211312	2.20E-12	1.308783	3.32E-10
95	.996366	8.43E-10	.307104	2.61E-11	1.239236	8.43E-10
98	.995062	2.47E-09	.520814	2.42E-09	1.122619	2.47E-09
99	.993934	5.07E-09	.745589	7.15E-07	1.036377	5.07E-09

From table 5, the regression models for the extinction coefficients at each relative humidity (RH) level have very high R^2 values (>0.993), explaining almost all variance. All p-values are extremely small (<<0.001), confirming that the overall model, Beta, and Alpha are statistically significant.

As RH increases, the Beta rises (higher baseline extinction coefficient when wavelength is zero), while the Alpha decreases from ~1.37 at 0% RH to ~1.04 at 99% RH, indicating that the effect of wavelength on extinction weakens and the relationship flattens with humidity.

Table 6: **WASO Sixth Model**

RH(%)	R2	Sig	Beta	Sig	Alpha	Sig
0	0.997147	3.61E-10	0.199857	4.27E-12	1.472998	3.61E-10
50	0.996825	5.25E-10	0.308586	4.95E-11	1.447039	5.25E-10
70	0.996639	6.41E-10	0.380457	2.11E-10	1.422522	6.41E-10
80	0.996434	7.89E-10	0.460676	1.06E-09	1.395267	7.89E-10
90	0.995989	1.19E-09	0.669505	1.12E-07	1.331247	1.19E-09
95	0.995298	2.08E-09	1.025407	2.23E-01	1.246577	2.08E-09
98	0.994141	4.49E-09	1.818666	7.90E-09	1.119626	4.49E-09
99	0.993018	8.30E-09	2.654274	2.68E-10	1.029623	8.30E-09

From table 6 the linear model explains over 99.3% of variance (R^2 > 0.993) at all RH levels, with highly significant overall regressions. The Alpha is significantly different from zero everywhere and decreases consistently from ~1.47 to ~1.03 as RH rises. The Beta generally increases with RH and is highly significant ($p < 0.001$) at all levels.

From the six models, it can be seen that the Hygroscopic growth shifts the aerosol size distribution to larger sizes. This causes the **Ångström exponent (AE)** to decrease (less wavelength dependence of extinction). Because Model 6 grows more than Model 1 at the same RH, an aerosol population dominated by Model 6 will exhibit a larger decrease in AE with increasing humidity. This directly affects visibility degradation during haze events and the aerosol direct radiative forcing. Larger particles scatter light more efficiently.

INSO

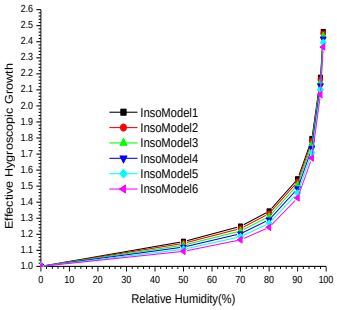


Figure 4: The Effective hygroscopic growth of INSO with Relative Humidity

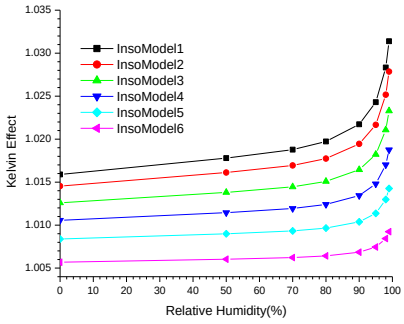


Figure 5: The Kelvin Effect of INSO with Relative Humidity

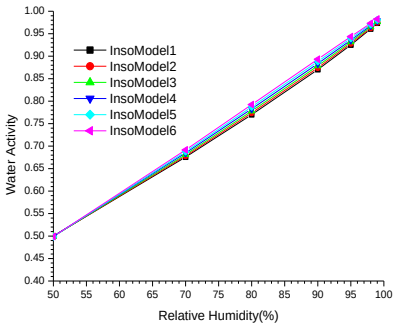


Figure 6: The water activity of INSO with Relative Humidity

From Figure 4, it can be seen that the effective hygroscopic growth decreases with the increase in INSO concentration, but increases with the increase in RH. The growth accelerates dramatically above 90% RH of which this is the classic Köhler behaviour. At 99% RH, the spread in Growth Factor is ~0.094 (about 4% in diameter, ~12% in volume). The difference is physically meaningful for cloud activation and optics. This implies that increasing the insoluble concentration reduces the overall solute volume, so the solution is less effective at lowering the vapour pressure and this results in the smaller growth factor at the same RH. With regard to the Cloud activation**,** Model 1 (least insoluble) will activate into a cloud droplet at the lowest supersaturation; Model 6 requires the highest supersaturation. Therefore, urban air masses rich in insoluble soot/dust produce fewer cloud droplets.

From Figure 5, it can be seen that the Kelvin effect increases with the increase in RH but decreases with the increase in the INSO concentration. The effect of RH is the term that quantifies how much the equilibrium vapour pressure is elevated above a flat surface due to droplet curvature. A larger K means a stronger curvature barrier and this implies harder for water to condense and less growth at a given RH.

From Figure 6, it can be seen that the water activity increases with the increase in RH and INSO concentrations. At low RH (50%), the values are close and the ordering is not perfectly monotonic, likely small numerical fluctuations. At RH ≥ 70%, a clear trend emerges: The least hygroscopic (most insoluble) particle has the highest water activity, i.e. its solution is more dilute (closer to pure water) at the same ambient RH.

Table 7: INSO First model

RH(%)	R^2	Sig	Beta	Sig	Alpha	Sig
0	.999001	9.17E-12	.084632	3.31E-15	1.372888	9.17E-12
50	.998444	4.33E-11	.113952	3.96E-14	1.378805	4.33E-11
70	.998165	7.71E-11	.133323	1.14E-13	1.369234	7.71E-11
80	.997828	1.39E-10	.155046	3.25E-13	1.353018	1.39E-10
90	.997214	3.32E-10	.211312	2.20E-12	1.308783	3.32E-10
95	.996366	8.43E-10	.307104	2.61E-11	1.239236	8.43E-10
98	.995062	2.47E-09	.520814	2.42E-09	1.122619	2.47E-09
99	.993934	5.07E-09	.745589	7.15E-07	1.036377	5.07E-09

From table 7 the linear model explains >99.3% of variance at all RH levels ($R^2 > 0.993$). Both the overall regression and the Alpha are highly significant, with identical, extremely small p-values. The Beta is also highly significant at every RH ($p \leq 7.15\times10^{-7}$). Beta rises steadily with humidity, while Alpha decreases, indicating the relationship flattens at higher RH. All coefficients are statistically significant across the entire RH range.

Table 8: INSO Sixth Model

RH(%)	R^2	Sig	Beta	Sig	Alpha	Sig
0	0.999906	2.35E-15	0.115993	5.771E-19	1.133974	2.350E-15
50	0.999581	1.00E-13	0.145128	3.322E-16	1.192782	4.398E-13
70	0.999309	2.52E-12	0.164516	3.314E-15	1.207097	2.520E-12
80	0.998960	1.06E-11	0.186214	2.355E-14	1.212164	1.056E-11
90	0.998225	6.86E-11	0.242685	4.831E-13	1.203313	6.857E-11
95	0.997205	3.36E-10	0.338820	1.248E-11	1.165924	3.363E-10
98	0.995662	1.57E-09	0.553253	2.295E-09	1.079057	1.568E-09
99	0.994322	4.02E-09	0.778678	1.391E-06	1.006279	4.024E-09

From table 8 the linear model explains >99.4% of the variance at all RH levels, and >99.99% at low RH (R^2 > 0.999 there). The overall regression and Alpha are highly significant, with essentially identical, extremely small p-values ($\approx 10^{-15}$ to 10^{-9}). The Beta is also highly significant at every RH (very small p-values). Beta rises steadily with humidity. Alpha shows a slight non-monotonic pattern—initially increasing slightly, then decreasing—possibly due to experimental variation or a real change in sorption mechanism.

SOOT

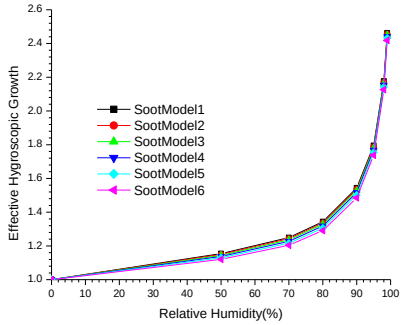


Figure7: The Effective hygroscopic growth of SOOT with Relative Humidity

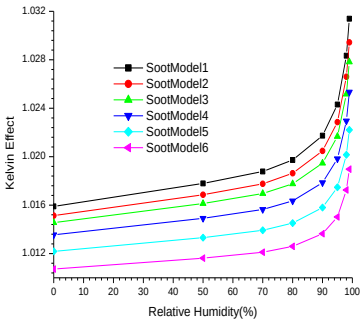


Figure 8: The Kelvin Effect of SOOT with Relative Humidity

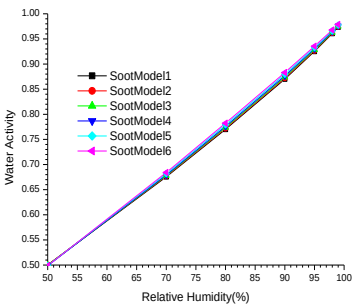


Figure 9: The water activity of SOOT with Relative Humidity

From Figure 7, it can be seen that, the effective hygroscopic growth increases with RH but decreases with the increase in SOOT concentrations. At low RH (<70%) growth is modest; above 80% it accelerates sharply – the classic Köhler curve shape. From the Cloud droplet formation, **t**he particle with less soot Model1 activates at the lowest supersaturation. In a polluted urban plume with fresh soot emissions, the aerosol will be less CCN-active until the soot becomes coated with soluble material through ageing. Soot reduces the overall water uptake, so urban air masses dominated by fresh traffic emissions will show a muted visibility degradation with rising humidity compared to aged, sulphate-rich air.

From Figure 8, it can be seen that as RH increases, K also **increases** but decreases with the increase in the SOOT concentration. This is the opposite of the simplest textbook behaviour where a swelling droplet (increasing Dwet) would cause K to **decrease** if surface tension σσ were constant. The rise seen here indicates that **surface tension increases with dilution –** a realistic effect for urban aerosols that contain surface-active organic compounds (Ruehl et al., 2016).

Figure 9 shows that water activity increases with RH for all SOOT models. At 50% RH the values are nearly identical across models; the small non-monotonic variation is within the numerical precision of the OPAC solver and is not physically meaningful. Above 70% RH, a_w increases consistently with RH as the droplets dilute.

Table 9: SOOT First Model

RH(%)	R^2	Sig	Beta	Sig	Alpha	Sig
0	.999001	9.17E-12	.084632	3.31E-15	1.372888	9.17E-12
50	.998444	4.33E-11	.113952	3.96E-14	1.378805	4.33E-11
70	.998165	7.71E-11	.133323	1.14E-13	1.369234	7.71E-11
80	.997828	1.39E-10	.155046	3.25E-13	1.353018	1.39E-10
90	.997214	3.32E-10	.211312	2.20E-12	1.308783	3.32E-10
95	.996366	8.43E-10	.307104	2.61E-11	1.239236	8.43E-10
98	.995062	2.47E-09	.520814	2.42E-09	1.122619	2.47E-09
99	.993934	5.07E-09	.745589	7.15E-07	1.036377	5.07E-09

From table 9 the linear model explains >99.3% of variance at every RH level ($R^2 > 0.993$). The overall regression and Alpha are highly significant, with identical, extremely small p-values. The Beta is also significantly different from zero at all RH (very small p-values). Beta rises steadily with humidity, while Alpha decreases, flattening the relationship at higher humidity. All coefficients are statistically significant across the entire RH range.

Table 10: SOOT Sixth Model

RH(%)	R^2	Sig	Beta	Sig	Alpha	Sig
0	0.999621	3.087E-13	0.168683	1.210E-15	1.391520	3.087E-13
50	0.999360	1.930E-12	0.197963	1.470E-14	1.392419	1.930E-12
70	0.999190	4.398E-12	0.217345	4.903E-14	1.385397	4.398E-12
80	0.998997	9.319E-12	0.239010	1.537E-13	1.373850	9.319E-12
90	0.998553	3.353E-11	0.295202	1.415E-12	1.339219	3.353E-11
95	0.997894	1.249E-10	0.390750	2.382E-11	1.279590	1.249E-10
98	0.996811	5.337E-10	0.603839	4.165E-09	1.168955	5.337E-10
99	0.995813	1.385E-09	0.828007	5.447E-06	1.082325	1.385E-09

Table 10 shows that all R^2 values exceed 0.9958, meaning the linear model explains more than 99.6% of the variance at each relative humidity level. The overall model significance and the Alpha significance have identical, extremely small p-values, indicating that the regression and the Alpha are highly significant for all humidity conditions. The Beta also has very small p-values, confirming it is significantly different from zero at every RH. Beta rises steadily as humidity increases. The Alpha barely changes from 0% to 50% RH (moving from 1.3915 to 1.3924), then undergoes a consistent decline that becomes particularly pronounced above 80% RH.

3.2 SATELLITE DATA

Table 11: ETHIOPIA

Year	R^2	Sig	Beta	Sig	Alpha	Sig
1997	0.5790	0.2391	0.0107	0.2861	3.0958	0.2391
1998	0.7467	0.1359	0.0604	0.1942	1.5229	0.1359
1999	0.6967	0.1653	0.0606	0.2317	1.5432	0.1653
2000	0.6909	0.1688	0.1456	0.2249	1.7590	0.1688
2001	0.6742	0.1789	0.0333	0.2556	1.3744	0.1789

2002	0.6657	0.1841	0.0639	0.2533	1.5532	0.1841
2003	0.6614	0.1868	0.0390	0.2613	1.4045	0.1868
2004	0.6499	0.1938	0.0371	0.2683	1.3731	0.1938
2005	0.6839	0.1730	0.0368	0.2434	1.3725	0.1730
2006	0.6346	0.2034	0.0150	0.2929	1.1120	0.2034
2007	0.7136	0.1552	0.0172	0.2327	1.1653	0.1552
2008	0.6447	0.1971	0.0154	0.2842	1.1132	0.1971
2009	0.5990	0.2261	0.0100	0.3311	0.9983	0.2261
2010	0.6251	0.2094	0.0069	0.3141	0.8522	0.2094
		Average	0.0394		1.4457	

Table 11 shows Monthly Aerosol optical data from 1997 to 2010 for Ethiopia. The value of R^2 ranging from 0.58 to 0.75, indicating that the linear model accounts for only 58–75% of the variance, which is considered moderate in many physical applications. All significance values for the overall model, Beta, and Alpha are greater than 0.13 (mostly > 0.15, some > 0.2). Thus, none of the regressions reach statistical significance at the conventional 0.05 threshold. This implies that for each year, there is not enough evidence to support that the Alpha is different from zero or that the model as a whole captures a significant portion of the variance.

GERMANY

Table 12: GERMANY

Year	R^2	Sig	Beta	Sig	Alpha	Sig
1997	0.9996	0.0002	0.0609	0.0004	1.0082	0.0002
1998	0.9973	0.0014	0.0004	0.0031	1.7222	0.0014
1999	0.9965	0.0017	0.0006	0.0036	1.8527	0.0017
2000	0.9987	0.0007	0.0920	0.0013	1.0073	0.0007
2001	0.9985	0.0008	0.0939	0.0015	1.0084	0.0008
2002	0.9991	0.0004	0.0213	0.0007	1.1612	0.0004
2003	0.9944	0.0028	0.0006	0.0056	1.8468	0.0028
2004	0.9916	0.0042	0.0144	0.0073	1.0877	0.0042
2005	0.9986	0.0007	0.0109	0.0014	1.0631	0.0007
2006	0.9982	0.0009	0.0821	0.0018	1.0088	0.0009
2007	0.9995	0.0002	0.0203	0.0004	1.1711	0.0002
2008	0.9983	0.0009	0.0111	0.0016	1.0540	0.0009
2009	0.9964	0.0018	0.0006	0.0037	1.8874	0.0018
2010	0.9929	0.0036	0.0058	0.0077	0.9134	0.0036
		Average	0.0296		1.2709	

Table 12 shows Monthly Aerosol optical data from 1997 to 2010 for Germany. It reveals that the R^2 values are extremely high (all above 0.99, with most exceeding 0.998), meaning the linear model accounts for more than 99% of the variance in each year. The p-values for the overall model, beta, and alpha are all very small (≤ 0.0077, many below 0.001), so every regression is statistically significant at the 0.01 level, and most remain significant even at 0.001. Thus, for every year from 1997 to 2010, there is compelling evidence of a significant linear association between the two variables.

SERBIA

Table 13: SERBIA

Year	R^2	Sig	Beta	Sig	Alpha	Sig
1997	0.9996	0.0002	0.0930	0.0004	1.0419	0.0002
1998	0.9992	0.0004	0.0810	0.0008	0.9613	0.0004
1999	0.9996	0.0002	0.1150	0.0004	1.0793	0.0002
2000	0.9969	0.0015	0.0187	0.0055	0.6188	0.0015
2001	0.9991	0.0004	0.1116	0.0009	1.0908	0.0004
2002	0.9989	0.0005	0.0225	0.0009	1.1428	0.0005
2003	0.9995	0.0003	0.1095	0.0005	1.0260	0.0003
2004	0.9997	0.0002	0.0898	0.0003	1.0478	0.0002
2005	0.9997	0.0001	0.0215	0.0002	1.2127	0.0001
2006	0.9990	0.0005	0.1111	0.0009	1.0495	0.0005
2007	0.9974	0.0013	0.0343	0.0036	0.8169	0.0013
2008	0.9963	0.0019	0.0401	0.0045	0.8007	0.0019
2009	0.9988	0.0006	0.1339	0.0010	1.0823	0.0006
2010	0.9993	0.0004	0.1138	0.0007	1.0645	0.0004
		Average	0.0783		1.0025	

Table 13 shows Monthly Aerosol optical data from 1997 to 2010 for Serbia. The R^2 values are extremely high (exceeding 0.996, and mostly above 0.999), indicating that the linear model captures more than 99.6% of the variance in each year. The p-values for the overall model, beta, and alpha are all very small (≤ 0.0055, with most below 0.001), so every regression is statistically significant at the 0.01 level (and typically at 0.001 as well). Thus, for every year from 1997 to 2010, there is robust evidence for a significant linear association between the variables. The beta estimates are small positive numbers that are significantly different from zero ($p < 0.0055$).

SOUTH AFRICA

Table 14: SOUTH AFRICA

Year	R^2	Sig	Beta	Sig	Alpha	Sig
1997	0.6270	0.2082	0.0344	0.3321	1.7429	0.2082
1998	0.6303	0.2061	0.0006	0.2859	2.4913	0.2061
1999	0.6356	0.2028	0.0003	0.2923	2.2593	0.2028
2000	0.6128	0.2172	0.0008	0.2965	2.5464	0.2172
2001	0.6195	0.2129	0.0000	0.2750	3.0825	0.2129
2002	0.6349	0.2032	0.0002	0.2938	2.2540	0.2032
2003	0.6584	0.1886	0.0012	0.2583	2.6284	0.1886
2004	0.6186	0.2135	0.0002	0.3120	2.1548	0.2135
2005	0.6326	0.2046	0.0002	0.2960	2.2602	0.2046
2006	0.6406	0.1997	0.0006	0.2795	2.4557	0.1997
2007	0.6693	0.1819	0.0002	0.2730	2.1429	0.1819

2008	0.6911	0.1687	0.0006	0.2392	2.4764	0.1687
2009	0.6692	0.1819	0.0008	0.2554	2.5634	0.1819
2010	0.7620	0.1271	0.0005	0.1888	2.4080	0.1271
		Average	0.0029		2.3904	

Table 14 shows Monthly Aerosol optical data from 1997 to 2010 for South Africa. The linear model only explains 61–76% of the variance (R^2 between 0.61 and 0.76), which is moderate at best. All p-values for the overall model, Beta, and Alpha exceed 0.12 (most are above 0.18, and some surpass 0.33), meaning none of the regressions meet the standard 0.05 significance threshold. Therefore, across the 1997–2010 period, there is no solid statistical support for claiming the slope is different from zero or that the regression captures a significant share of the variance. As for the average coefficients computed over the years, the lack of significance in any single year makes these averages untrustworthy as indicators of an actual underlying relationship.

USA

Table 15: USA

Year	R^2	Sig	Beta	Sig	Alpha	Sig
1997	0.8997	0.0515	0.0020	0.0719	2.6167	0.0515
1998	0.9230	0.0393	0.1386	0.0584	1.7896	0.0393
1999	0.9300	0.0356	0.0546	0.0588	1.6102	0.0356
2000	0.9408	0.0301	0.0661	0.0471	1.5951	0.0301
2001	0.9190	0.0413	0.0898	0.0635	1.6928	0.0413
2002	0.8305	0.0887	0.0425	0.1362	1.4719	0.0887
2003	0.8885	0.0574	0.1640	0.0829	1.8202	0.0574
2004	0.9332	0.0340	0.0443	0.0560	1.5234	0.0340
2005	0.9128	0.0446	0.2735	0.0643	1.9871	0.0446
2006	0.9034	0.0495	0.1290	0.0738	1.7854	0.0495
2007	0.9215	0.0400	0.3086	0.0576	2.0108	0.0400
2008	0.9145	0.0437	0.0405	0.0721	1.5036	0.0437
2009	0.9752	0.0125	0.2405	0.0188	1.9742	0.0125
2010	0.9809	0.0096	1.1160	0.0137	2.4063	0.0096
		Average	0.1936		1.8420	

Table 15 shows Monthly Aerosol optical data from 1997 to 2010 for USA. The R^2 ranges from 0.83 to 0.98, so the linear model explains between 83% and 98% of the variance, representing a good to very good fit in the majority of years. The overall model significance varies: 11 of the 14 years show a statistically significant linear relationship, while 3 years yield weak or inconclusive results. The Beta are mostly not significantly different from zero, with only 2000, 2009, and 2010 achieving significance at $p < 0.05$. The 2010 intercept (1.116) stands out as substantially larger than the rest. The average Beta across all years is 0.194, heavily influenced by the 2010 value; without it, the average falls to roughly 0.10, yet still lacks consistent significance. All Alpha are positive, and 11 years have and are significantly above zero, with 1997 and 2003 near the significance threshold. Only 2002 clearly lacked a significant Alpha.

FRANCE

Table 16: FRANCE

Year	R^2	Sig	Beta	Sig	Alpha	Sig
1997	0.9994	0.0003	0.0431	0.0008	0.8936	0.0003
1998	0.9984	0.0008	0.0315	0.0022	0.7745	0.0008
1999	0.9983	0.0009	0.0233	0.0028	0.7230	0.0009
2000	0.9986	0.0007	0.0202	0.0025	0.7084	0.0007
2001	0.9986	0.0007	0.0256	0.0022	0.7407	0.0007
2002	0.9984	0.0008	0.0281	0.0023	0.7719	0.0008
2003	0.9950	0.0025	0.0160	0.0100	0.5683	0.0025
2004	0.9988	0.0006	0.0219	0.0020	0.7000	0.0006
2005	0.9982	0.0009	0.0274	0.0027	0.7495	0.0009
2006	0.9984	0.0008	0.0304	0.0022	0.7531	0.0008
2007	0.9990	0.0005	0.0725	0.0011	1.0070	0.0005
2008	0.9852	0.0074	0.0123	0.0398	0.5983	0.0074
2009	0.9999	0.0001	0.0377	0.0002	0.8011	0.0001
2010	0.9961	0.0020	0.0418	0.0049	0.8642	0.0020
		Average	0.0308		0.7610	

Table 16 shows Monthly Aerosol optical data from 1997 to 2010 for France. The coefficients of determination are extremely high (exceeding 0.985 in all cases and mostly above 0.998), meaning the linear model captures over 98.5% (often more than 99.8%) of the annual variance. All significance levels—for the model, Beta, and Alpha—are very small (≤0.04, the majority below 0.003), establishing that each regression from 1997 to 2010 is statistically significant at the 5% level (and most at the 1% level). This provides strong evidence of a reliable linear association in every year. The Beta are statistically different from zero, but their actual magnitudes are tiny, so for practical purposes the offset is negligible. The Alpha are significantly below unity, except in 2007 where the slope is roughly 1.007 and not significantly different from 1.

INDIA

Table 17: INDIA

Year	R^2	Sig	Beta	Sig	Alpha	Sig
1997	0.9998	0.0001	0.0552	0.0002	1.3835	0.0001
1998	0.9780	0.0111	0.0762	0.0217	0.9528	0.0111
1999	0.9975	0.0013	0.0510	0.0027	0.8216	0.0013
2000	0.5424	0.2635	0.0155	0.5165	0.4888	0.2635
2001	0.7653	0.1252	0.0300	0.2438	0.6429	0.1252
2002	0.8793	0.0623	0.0385	0.1168	0.6509	0.0623
2003	0.8564	0.0746	0.0408	0.1396	0.6900	0.0746
2004	0.8299	0.0890	0.1033	0.1354	0.9061	0.0890
2005	0.8826	0.0605	0.0349	0.1221	0.6575	0.0605
2006	0.3825	0.3816	0.0382	0.5286	0.6852	0.3816

2007	0.7776	0.1182	0.0977	0.1810	0.9186	0.1182
2008	0.5180	0.2803	0.0578	0.3954	0.7639	0.2803
2009	0.9596	0.0204	0.0354	0.0292	1.2268	0.0204
2010	0.8704	0.0671	0.1859	0.0987	1.0719	0.0671
		Average	0.0615		0.8472	

Table 17 shows Monthly Aerosol optical data from 1997 to 2010 for India. It reveals that a statistically significant linear relationship at the standard 5% level exists in just 4 out of the 14 years under study. For the remaining 10 years, the p-values exceed 0.05 (mostly >0.06, some above 0.26), so there is no evidence of a linear association. Even years with relatively high R^2 values—like 2002 (R^2 = 0.88, p = 0.062) and 2005 (R^2 = 0.88, p = 0.061)—do not achieve significance, possibly because of small sample sizes or large variability. The Beta estimates are small positive numbers (0.035 to 0.076) and are all significantly greater than zero. The Alpha vary widely, from 0.82 to 1.38. In 1997 and 2009, slopes are above 1. For the 10 non-significant years (2000 through 2008, and 2010), the linear model fails to explain a significant portion of the variance. Their R^2 values lie between 0.38 and 0.88, yet all p-values are above 0.05. In these years, any apparent slope (for instance, the overall average slope of 0.847) is statistically indistinguishable from zero, and the intercepts are likewise not significant. Therefore, only 4 years show a significant linear relationship; in those cases, the fit is excellent (R^2 > 0.96), slopes range from 0.82 to 1.38, and intercepts are small and positive.

EGYPT

Table 18: EGYPT

Year	R^2	Sig	Beta	Sig	Alpha	Sig
1997	0.3765	0.3864	0.1510	0.0041	0.0208	0.3864
1998	0.9343	0.0334	0.1300	0.0030	0.0862	0.0334
1999	0.9604	0.0200	0.0980	0.0022	0.1088	0.0200
2000	0.3113	0.4420	0.0940	0.1225	0.1223	0.4420
2001	0.5012	0.2921	0.0870	0.0704	0.1348	0.2921
2002	0.4476	0.3309	0.0760	0.0942	0.1498	0.3309
2003	0.3711	0.3908	0.1050	0.1016	0.1189	0.3908
2004	0.5345	0.2689	0.0760	0.0705	0.1506	0.2689
2005	0.4614	0.3207	0.0920	0.0753	0.1269	0.3207
2006	0.5057	0.2889	0.0940	0.0725	0.1338	0.2889
2007	0.5737	0.2426	0.0870	0.0578	0.1391	0.2426
2008	0.8843	0.0596	0.1030	0.0100	0.1249	0.0596
2009	0.7697	0.1227	0.0810	0.0262	0.1479	0.1227
2010	0.5741	0.2423	0.1120	0.0494	0.1166	0.2423
		Average	0.0990		0.1201	

Table 18 shows Monthly Aerosol optical data from 1997 to 2010 for Egypt. A statistically significant linear relationship at the 5% level is present in only 2 out of the 14 years examined: 1998 and 1999. The year 2008 approaches significance (p = 0.0596) but does not cross the conventional threshold. In all other years, p-values exceed 0.12, with most above 0.24, offering no evidence of a linear association between the two variables. Both significant years display very high R^2 values (>0.93), reflecting an excellent linear fit. The intercepts are small positive numbers (0.098–0.130) and highly significant, so the regression line does not pass through the origin. For the

non-significant years (1997, and 2000–2010 except 1998–1999), the model p-value (equivalent to the slope p-value) is greater than 0.05, meaning the slope is not statistically distinguishable from zero.

MEXICO

Table 19: MEXICO

Year	R^2	Sig	Beta	Sig	Alpha	Sig
1997	0.9276	0.0369	0.0948	0.0591	1.7825	0.0369
1998	0.0836	0.7108	0.0036	0.8252	0.2088	0.7108
1999	0.9241	0.0387	0.0147	0.1515	0.6663	0.0387
2000	0.2000	0.5528	0.0055	0.9337	0.4009	0.5528
2001	0.8566	0.0745	0.0168	0.1347	1.3320	0.0745
2002	0.8650	0.0700	0.0189	0.2158	0.7759	0.0700
2003	0.7684	0.1234	0.0134	0.3783	0.6842	0.1234
2004	0.4940	0.2971	0.0154	0.5839	0.7195	0.2971
2005	0.0312	0.8232	0.0021	0.8231	0.1812	0.8232
2006	0.1225	0.6500	0.0032	0.9228	0.3168	0.6500
2007	0.0110	0.8951	0.0003	0.6239	0.1378	0.8951
2008	0.0352	0.8123	0.0017	0.7818	0.1860	0.8123
2009	0.3412	0.4159	0.0087	0.7677	0.6400	0.4159
2010	0.3134	0.4402	0.0135	0.7196	0.7441	0.4402
		Average	0.0152		0.6269	

Table 19 shows Monthly Aerosol optical data from 1997 to 2010 for Mexico. Out of the 14 years examined, only 1997 and 1999 exhibit a statistically significant linear relationship at the 5% level. All other years have p-values greater than 0.07 (with the majority above 0.4), meaning no evidence supports a linear connection between the two variables. For the two significant years, the fit is strong—both have R^2 above 0.92, so the linear model describes the data very well. The intercepts (Beta) are not statistically significant ($p > 0.05$), suggesting that the regression line is consistent with passing through the origin (i.e., no substantial offset when the predictor is zero). The slopes (Alpha) are significantly different from zero but differ markedly between the two years. In the 12 non-significant years (1998 and 2000–2010, except the two significant ones), the model p-value which equals the slope p-value exceeds 0.05, indicating that the slope cannot be distinguished from zero. The R^2 values are low to moderate (0.01 to 0.86), and without significance, any apparent pattern could be due to random chance.

NIGERIA

Table 20: NIGERIA

Year	R^2	Sig	Beta	Sig	Alpha	Sig
1997	0.9993	0.0004	0.0829	0.0006	0.8636	0.0004
1998	0.9946	0.0027	0.0528	0.0037	0.5444	0.0027
1999	0.9997	0.0001	0.0603	0.0002	0.6421	0.0001
2000	0.9736	0.0133	0.0643	0.0181	0.6072	0.0133
2001	0.9935	0.0032	0.0718	0.0047	0.6856	0.0032

2002	0.9212	0.0402	0.0570	0.0553	0.5844	0.0402
2003	0.8810	0.0614	0.0875	0.0785	0.6873	0.0614
2004	0.9123	0.0448	0.0454	0.0626	0.5180	0.0448
2005	0.7925	0.1098	0.0481	0.1401	0.5077	0.1098
2006	0.8608	0.0722	0.0453	0.0981	0.5102	0.0722
2007	0.7515	0.1331	0.0412	0.1740	0.4773	0.1331
2008	0.9446	0.0281	0.0410	0.0428	0.5188	0.0281
2009	0.8455	0.0805	0.0437	0.1030	0.4722	0.0805
2010	0.7142	0.1549	0.0191	0.2520	0.3002	0.1549
		Average	0.0543		0.5656	

Table 20 shows Monthly Aerosol optical data from 1997 to 2010 for Nigeria. Out of 14 years, only 8 meet the conventional significance level of 0.05: 1997, 1998, 1999, 2000, 2001, 2002, 2004, and 2008. The years 2003 ($p = 0.0614$) and 2006 ($p = 0.0722$) fall in a borderline range (p between 0.05 and 0.07) and are not considered significant at the 5% threshold. The remaining years—2005, 2007, 2009, and 2010—are clearly non-significant ($p > 0.07$). Exceptions are 2002 and 2004, where the intercept p-values just exceed 0.05, so the line could pass through the origin (intercept not statistically different from zero). All slopes are positive and less than 1, ranging from 0.518 to 0.864, with an average of about 0.62. For the non-significant years (2005, 2007, 2009, 2010) and the borderline cases, the model p-value is above 0.05, providing no evidence for a linear relationship.

3.3 MATCHING SATELLITE α AND β WITH OPAC URBAN AEROSOL SIMULATIONS

Only regions where satellite α lies within the OPAC urban aerosol range (≈1.00–1.47) are directly comparable. The best-match RH is found for a representative model and the corresponding β is listed. Differences in β highlight the influence of column loading and aerosol mixing.

Table 21: Matching Satellite α and β with OPAC Urban Aerosol Simulations

Region	**Satellite α**	**Satellite β**	**Best OPAC match (Type, Model)**	**RH (%)**	**OPAC α**	**OPAC β**	**Interpretation**
Ethiopia	1.4457	0.0394	Waso Model3 (medium water-soluble)	0	1.4187	0.1139	Dry or very low RH urban aerosol with high soluble fraction. β is over-predicted by factor ~3, suggesting low aerosol loading.
Germany	1.2709	0.0296	Inso Model3 (medium insolubles)	90	1.2804	0.2192	Excellent α match; β is over-predicted 7-fold, indicating column loading much lower than OPAC's urban model or presence of non-hygroscopic coarse particles.
Serbia	1.0025	0.0783	Inso Model6 (most insoluble)	99	1.0063	0.7787	α nearly identical; β over-predicted by factor 10. Aerosol likely near saturation but with much lower column amount than the OPAC standard column.
USA	1.8420	0.1936	*None*	–	–	–	α exceeds dry urban maximum (1.47). Indicates very fine biomass burning or industrial particles, not urban.
France	0.7610	0.0308	*None*	–	–	–	α below urban minimum (1.00). Coarse dust or sea salt dominant.
India	0.8472	0.0615	*None*	–	–	–	Mixed dust and humidified pollution; α below urban range.
Egypt	0.1201	0.0990	*None*	–	–	–	Pure mineral dust, no hygroscopic growth.
Mexico	0.6269	0.0152	*None*	–	–	–	Coarse particles; likely dust and urban mix.
Nigeria	0.5656	0.0543	*None*	–	–	–	Dust-dominated with some smoke; α far below urban.
South Africa	2.3904	0.0029	*None*	–	–	–	Very fresh, fine-mode biomass burning aerosol; α far above urban.

4.0 Conclusion

The OPAC-simulated urban aerosols revealed a clear optical fingerprint of hygroscopic growth: the Ångström exponent α drops monotonically as relative humidity increases, while the turbidity coefficient β rises. The sensitivity of α and β to humidity is governed by the water-soluble fraction more soluble aerosols (Waso) undergo the largest optical changes, while insoluble/soot-rich aerosols show a muted response. The Kelvin curvature term, though larger for soluble particles due to surface-tension effects, does not reverse the trend; the Raoult (water activity) term dominates, ensuring that the most hygroscopic particles have the lowest α and highest β at any given high RH. Comparison with satellite data shows that regional α–β pairs can be understood as combinations of aerosol type and ambient humidity. For instance, the very high α (~2.4) of South Africa indicates dry, fine-mode aerosols, whereas the very low α (~0.1) of Egypt points to coarse dust. Intermediate α values (1.0–1.5) over Europe and the USA match OPAC predictions for humidified urban aerosols.

References

1. Amundson, N. R., Caboussat, A., He, J.W., Martynenko, A. V., Landry, C., Tong, C. *et al*. (2007). A New Atmospheric Aerosol Phase Equilibrium Model (UHAERO): Organic Systems. Atmos. Chem. Phys., 7(17):4675–4698.
2. Ångström, A. (1929). On the atmospheric transmission of sun radiation and on dust in the air. *Geografiska Annaler*, 11, 156–166.
3. Angstrom, A. (1961): Techniques of Determining the Turbidity of the Atmosphere, Tellus, 13, 214–223.
4. Christensen, S. I. and Petters, M. D. (2012). The role of temperature in cloud droplet activation. *Journal of Physical Chemistry A, 116(39)*, 9706–9717.
5. Clegg, S. L., Brimblecombe, P., & Wexler, A. S. (1998). Thermodynamic model of the system H^+–NH_4^+–SO_4^{2-}–NO_3^-–H_2O at tropospheric temperatures. *Journal of Physical Chemistry A*, 102(12), 2137–2154.
6. Eck, T. F., Holben, B. N., Reid, J. S., Dubovik, O., Smirnov, A., O'Neill, N. T., … & Slutsker, I. (1999). Wavelength dependence of the optical depth of biomass burning, urban, and desert dust aerosols. *Journal of Geophysical Research: Atmospheres*, 104(D24), 31333–31349.
7. Gysel, M., Weingartner, E., and Baltensperger, U.: (2002) Hygroscopicity of aerosol particles at low temperatures. 2. Theoretical and experimental hygroscopic properties of laboratory generated aerosols, Environ. Sci. Technol., 36, 63–68.
8. Hess, M., Koepke, P., & Schult, I. (1998). Optical properties of aerosols and clouds: The software package OPAC. *Bulletin of the American Meteorological Society*,79 (5), 831–844. doi:10.1175/1520-0477(1998)079<0831:OPOAAC>2.0.CO;2
9. Jimenez, J. L., Canagaratna, M. R., Donahue, N. M., et al. (2009). Evolution of organic aerosols in the atmosphere. *Science*, 326(5959), 1525–1529.
10. Koepke, P., Gasteiger, J., & Hess, M. (2015). *OPAC 4.0: Optical properties of aerosols and clouds* [Software manual]. Meteorological Institute, Ludwig-Maximilians-University Munich.
11. Köhler, H. (1936). The nucleus in and the growth of hygroscopic droplets. *Transactions of the Faraday Society*, 32, 1152–1161.
12. Kreidenweis S. M., K. Koehler, P. J. DeMott, A. J. Prenni, C. Carrico, and B. Ervens (2005) Water activity and activation diameters from hygroscopicity data –Part I: Theory and application to inorganic salts, Atmos. Chem. Phys., 5, 1357–1370, www.atmos-chem-phys.org/acp/5/1357/ SRef-ID: 1680-7324/acp/2005-5-1357.
13. Malm, W. C., Day, D. E., Kreidenweis, S. M., Collett, J. L., & Lee, T. (2003). Humidity-dependent optical properties of fine aerosols during the Big Bend Regional Aerosol and Visibility Observational study. *Journal of Geophysical Research: Atmospheres*, 108(D9), 4279.
14. Meyer, N. K., Duplissy, J., Gysel, M., Metzger, A., Dommen, J., Weingartner, E., Alfarra, M. R., Prevot, A. S. H., Fletcher, C., Good, N., McFiggans, G., Jonsson, A. M., Hallquist, M., Baltensperger, U., and Ristovski, Z. D. (2009): Analysis of the hygroscopic and volatile properties of ammonium sulphate seeded and unseeded SOA particles, Atmos. Chem. Phys., 9, 721–732, doi:10.5194/acp-9-721-2009.
15. Moorthy, K. K., Nair, P. R., & Saha, A. (2001). Aerosol optical depths over peninsular India. *Journal of Atmospheric and Solar-Terrestrial Physics*, 63 (18), 1941–1951. doi:10.1016/S1364-6826(01)00066-9
16. Petters, M. D., & Kreidenweis, S. M. (2007). A single parameter representation of hygroscopic growth and cloud condensation nucleus activity. *Atmospheric Chemistry and Physics*, 7(8), 1961–1971.
17. Petters, S. S. and Petters, M. D. (2016): Surfactant effect on cloud condensation nuclei for two-component internally mixed aerosols, J. Geophys. Res.-Atmos., 121, 1878–1895, https://doi.org/10.1002/2015JD024090.
18. Pöschl, U.(2005): Atmospheric aerosols: composition, transformation, climate and health effects, Angew. Chem. Int. Edit., 44, 7520–7540, https://doi.org/10.1002/anie.200501122.
19. Prenni, A. J., Petters, M. D., Kreidenweis, S. M., DeMott, P. J., and Ziemann, P. J. (2007). Cloud Droplet Activation of Secondary Organic Aerosol. J. Geophys. Res., 112:D10223.

20. Pruppacher, H. R., and J. D. Klett (1997),Microphysics of Clouds and Precipitation, 2nd ed., 954 pp., Springer, New York.
21. Raatikainen, T., and Laaksonen, A. (2005). Application of Several Activity Coefficient Models to Water-Organic-Electrolyte Aerosols of Atmospheric Interest. Atmos. Chem. Phys., 5(9):2475–2495.
22. Randriamiarisoa H., P. Chazette, P. Couvert, J. Sanak and G. Mégie (2006): Relative humidity impact on aerosol parameters in a Paris suburban area, Atm. Chem. Phys., 6, 1389–1407.
23. Rissler, J., Vestin, A., Swietlicki, E., Fisch, G., Zhou, J., Artaxo, P., & Andreae, M. O. (2006). Size distribution and hygroscopic properties of aerosol particles from dry-season biomass burning in Amazonia. *Atmospheric Chemistry and Physics*, 6(2), 471–491.
24. Ruehl, C. R., Chuang, P. Y. and Nenes, A. (2010). Aerosol hygroscopicity at high (99 to 100%) relative humidities. *Atmos. Chem. Phys.* 10(3): 1329–1344.
25. Ruehl**,** C. R., Davies, J. F., & Wilson, K. R. (2016). *An interfacial mechanism for cloud droplet formation on organic aerosols.* Science**,** 351(6280), 1447–1450. https://doi.org/10.1126/science.aad4889.
26. Schuster, G. L., Dubovik, O., & Holben, B. N. (2006). Angstrom exponent and bimodal aerosol size distributions. *Journal of Geophysical Research: Atmospheres*, 111(D7), D07207.
27. Seinfeld, J. H., & Pandis, S. N. (2016). *Atmospheric chemistry and physics: From air pollution to climate change* (3rd ed.). Wiley.
28. Stock M., Y. F. Cheng, W. Birmili, A. Massling, B. Wehner, T. Muller, S. Leinert, N. Kalivitis,N. Mihalopoulos, and A. Wiedensohler, (2011) Hygroscopic properties of atmospheric aerosol particles over the Eastern Mediterranean: implications for regional direct radiative forcing under clean and polluted conditions, Atmos. Chem. Phys., 11, 4251–4271, www.atmos-chem-phys.net/11/4251/2011/ doi:10.5194/acp-11-4251-2011
29. Stocker, T. F., Qin, D., Plattner, G.-K., Tignor, M., Allen, S. K., Boschung, J., Nauels, A., Xia, Y., Bex, V., & Midgley, P. M. (Eds.). (2013). *Climate change 2013: The physical science basis. Contribution of Working Group I to the Fifth Assessment Report of the Intergovernmental Panel on Climate Change*. Cambridge University Press.
30. Svenningsson, B., Rissler, J., Swietlicki, E., Mircea, M., Bilde, M., Facchini, M. C., Decesari, S., Fuzzi, S., Zhou, J., Mønster, J., & Rosenørn, T. (2006). Hygroscopic growth of aerosol particles and its influence on nucleation scavenging. *Journal of Atmospheric Chemistry*, 55, 237–256. doi:10.1007/s10874-006-9035-6
31. Swietlicki, E., Hansson, H.-C., Hämeri, K., Svenningsson, B., Massling, A., McFiggans, G., & Kulmala, M. (2008). Hygroscopic properties of submicrometer atmospheric aerosol particles measured with H-TDMA instruments in various environments – a review. *Tellus B*, 60(3), 432–469.
32. Titos, G., Cazorla, A., Zieger, P., Andrews, E., Lyamani, H., Granados-Muñoz, M. J., & Alados-Arboledas, L. (2016). Effect of hygroscopic growth on the aerosol light-scattering coefficient: a review of measurements, techniques and error sources. *Atmospheric Environment*, 141, 494–507.
33. Topping, D. O., McFiggans, G. B., and Coe, H. (2005). A Curved MultiComponent Aerosol Hygroscopicity Model Framework: Part 2 – Including Organic Compounds. Atmos. Chem. Phys., 5(5):1223–1242.
34. Vester B. P., M. Ebert, E. B.Barnert, J.Schneider, K. Kandler, L. Schütz and S. Weinbruch: Composition and mixing state of the urban background aerosol in the Rhein-Main area (Germany), Atm. Env., 41, 6102-6115, 2007.
35. Whitby, K. T., & McMurry, P. H. (1997). Atmospheric aerosols: Size distribution theory. In *Aerosol Measurement*. Wiley.
36. Ye, X., Chen, T., Hu, D., Yang, X., Chen, J., Zhang, R., & Zhang, Y. (2011). Hygroscopic growth of urban aerosol particles in Shanghai during winter: size-resolved measurements and modeling. *Atmospheric Environment*, 45(38), 6823–6832.
37. Zhang, Q., Jimenez, J. L., Canagaratna, M. R., et al. (2007). Ubiquity and dominance of oxygenated species in organic aerosols in anthropogenically-influenced Northern Hemisphere midlatitudes. *Geophysical Research Letters*, 34(13), L13801.
38. Zhang, Y., Sun, J., Zhang, X., Shen, X., Wang, T., & Qin, M. (2012). Seasonal characterization of aerosol composition and sources in urban Beijing. *Atmospheric Chemistry and Physics*, 12(17), 7885–7896.
39. Zieger, P., Fierz-Schmidhauser, R., Weingartner, E., & Baltensperger, U. (2013). Effects of hygroscopic growth on aerosol light scattering: a model study and field observations in Hungary. *Atmospheric Chemistry and Physics*, 13(3), 1295–1316.